




ARTICLE OPEN



Nicotine dependence and insula subregions: functional connectivity and cue-induced activation

Dara G. Ghahremani^{1,6} , Jean-Baptiste F. Pochon^{1,6}, Maylen Perez Diaz¹, Rachel F. Tyndale^{2,3} , Andy C. Dean^{1,4} and Edythe D. London^{1,4,5} 

© The Author(s) 2023

Nicotine dependence is a major predictor of relapse in people with Tobacco Use Disorder (TUD). Accordingly, therapies that reduce nicotine dependence may promote sustained abstinence from smoking. The insular cortex has been identified as a promising target in brain-based therapies for TUD, and has three major sub-regions (ventral anterior, dorsal anterior, and posterior) that serve distinct functional networks. How these subregions and associated networks contribute to nicotine dependence is not well understood, and therefore was the focus of this study. Sixty individuals (28 women; 18–45 years old), who smoked cigarettes daily, rated their level of nicotine dependence (on the Fagerström Test for Nicotine Dependence) and, after abstaining from smoking overnight (~12 h), underwent functional magnetic resonance imaging (fMRI) in a resting state. A subset of these participants ($N = 48$) also completing a cue-induced craving task during fMRI. Correlations between nicotine dependence and resting-state functional connectivity (RSFC) and cue-induced activation of the major insular sub-regions were evaluated. Nicotine dependence was negatively correlated with connectivity of the left and right dorsal, and left ventral anterior insula with regions within the superior parietal lobule (SPL), including the left precuneus. No relationship between posterior insula connectivity and nicotine dependence was found. Cue-induced activation in the left dorsal anterior insula was positively associated with nicotine dependence and negatively associated with RSFC of the same region with SPL, suggesting that craving-related responsivity in this subregion was greater among participants who were more dependent. These results may inform therapeutic approaches, such as brain stimulation, which may elicit differential clinical outcomes (e.g., dependence, craving) depending on the insular subnetwork that is targeted.

Neuropsychopharmacology (2023) 48:936–945; <https://doi.org/10.1038/s41386-023-01528-0>

INTRODUCTION

The use of combustible tobacco products persists as a substantial public health problem, causing >7 million (or 1 in 10) deaths worldwide annually [1]. Among people who try to quit smoking independently, only 3–6% successfully stop for 6–12 months, and most fail within 8 days [2]. Behavioral and pharmacological treatments for Tobacco Use Disorder (TUD) yield limited success [3–5], highlighting a need for novel therapeutic strategies.

Nicotine dependence is a major predictor of relapse in people with TUD. Nicotine dependence measured using the Fagerström Test for Nicotine Dependence (FTND) [6] predicted relapse at 1- and 2-year follow up assessments [7]. In participants maintaining smoking abstinence for a month followed by behavioral and pharmacological therapy, relapse rates at 1-year follow up were higher among those with greater nicotine dependence [8] (measured with FTND). FTND also predicted the success of abstinence imposed by hospitalizations for cardiac problems [9, 10] or pregnancy [11]. These findings suggest that nicotine dependence may be a tangible therapeutic metric and target for

determining success in reduction of cigarette smoking or abstinence. Accordingly, elucidating the neural mechanisms of nicotine dependence has the potential to advance TUD treatment [12], particularly with neuroanatomically-based approaches, such as targeted brain stimulation [13, 14]. Further knowledge of the neural systems underlying nicotine dependence is critical for guiding these treatments.

The insula has been identified as a promising therapeutic target for TUD, partly due to clinical evidence for its role in smoking behavior [15, 16]. Patients with insula lesions resulting from strokes markedly reduced their smoking [17–19], and survivors of strokes with damage to the right insula maintained abstinence from smoking for >1 year after hospital discharge [18, 20].

Neuroimaging studies have also indicated the importance of the insula in maintenance of cigarette smoking. Cortical thickness of insular sub-regions is negatively related to nicotine dependence [21–23] and cigarette craving [24]. Resting-state functional connectivity (RSFC) has been used to assess neural systems involved in nicotine dependence [25, 26]. A negative relationship

¹Department of Psychiatry and Biobehavioral Sciences, Semel Institute for Neuroscience and Human Behavior, University of California, Los Angeles, CA, USA. ²Department of Pharmacology & Toxicology and Department of Psychiatry, University of Toronto, 1 King's College Circle, Toronto, ON, Canada. ³Campbell Family Mental Health Research Institute, Centre for Addiction and Mental Health, Toronto, ON, Canada. ⁴Brain Research Institute, University of California, Los Angeles, CA, USA. ⁵Department of Molecular and Medical Pharmacology, University of California, Los Angeles, CA, USA. ⁶These authors contributed equally: Dara G. Ghahremani, Jean-Baptiste F. Pochon. [✉]email: darag@ucla.edu; elondon@mednet.ucla.edu

Received: 17 May 2022 Revised: 29 December 2022 Accepted: 2 January 2023

Published online: 3 March 2023

was found between nicotine dependence and RSFC of the anterior cingulate cortex (ACC) with the striatum [27, 28]. Other RSFC studies showed an inverse relationship between nicotine dependence and insula-ACC connectivity [29–31]. Cue-induced craving paradigms have also been used to examine neural systems associated with nicotine dependence [32, 33]—one fMRI study showed a positive relationship between nicotine dependence and activation in the anterior and posterior insula in response to smoking-related cues. The particular insular subregions showing this relationship depended on the condition (e.g., baseline, food cues) used to contrast with the cues condition [32].

The insula has been subdivided into three major sub-regions that serve distinct functions: dorsal anterior, ventral anterior, and posterior [34, 35]. Whereas the posterior portion of the insula connects with sensorimotor integration areas (e.g., pre-motor, supplementary motor cortex), the anterior portion is functionally linked with limbic regions and is a key component of the “salience network”, which includes the ACC [36]. The anterior portion generally serves cognitive and affective functions [37, 38]. Further functional distinctions have been made between dorsal and ventral anterior insula connectivity along cognitive and affective domains, respectively [39, 40]. In addition, dorsal/ventral distinctions have been conceptualized as components of externally- and internally oriented networks—the frontoparietal attention network and the default mode network, respectively [41, 42]. These functional distinctions can be translated to different aspects of TUD. The posterior insula is considered a hub for primary convergence of interoceptive signals [43, 44]; thus, the sensorimotor integration functions of this subregion may be linked to interoceptive aspects of nicotine withdrawal symptoms and craving, especially somatosensory features of the latter. The dorsal/ventral anterior insula distinction along externally/internally oriented networks has been linked to cue-induced vs. spontaneous craving, respectively [42], providing evidence for subregional specificity for different dimensions of craving in TUD. Moreover, the cognitive/affective distinction of dorsal/ventral anterior insula suggests that these regions may differentiate cognitive aspects of the disorder (e.g., planning for the next cigarette) and emotional/affective aspects (e.g., negative affect associated with brief abstinence/withdrawal).

Given the functional heterogeneity of insular subregions, understanding the relationship of each subregion to nicotine dependence can advance efforts to refine neurotherapeutic targets for brain stimulation. The most common non-invasive brain stimulation technique used for TUD is transcranial magnetic stimulation (TMS), but studies of TMS on smoking behavior show weak or no effects [13, 45]. Such discrepancy may, in part, reflect the lack of spatial precision in the brain area stimulated by TMS, which produces stimulation in areas that span across insular subregions and into the prefrontal cortex. Other, more novel non-invasive brain stimulation techniques, such as low intensity focused ultrasound pulsation (LIFUP) [46], can target smaller brain structures and allow for more precise stimulation of insular subregions. However, a better understanding of the differences in these subregions with respect to nicotine dependence is needed to determine optimal insular stimulation targets.

Prior studies of RSFC have attempted to distinguish between connectivity of insular sub-regions with respect to smoking-related behavioral variables [30, 42, 47–49], but only two of them examined RSFC of insula subregions with respect to nicotine dependence [29, 30]. These studies showed negative relationships between connectivity of the dorsal ACC with anterior [29] and posterior [30] insula. Despite this initial evidence for distinctions between subregions, a comprehensive analysis of their contributions is lacking, leaving open the possibility that RSFC of different insular subregions are differentially related to nicotine dependence. We therefore undertook a comprehensive analysis of correlations with connectivity patterns of these insular subregions

in a whole-brain analysis. We also tested the relationship between nicotine dependence and activation of insula subregions during cue-induced craving for cigarettes and examined the relationship between this activation and insula RSFC.

In a group of 60 participants who smoked cigarettes daily and maintained overnight abstinence from smoking, we examined the relationship of nicotine dependence with RSFC and cue-induced activation (using task-based fMRI) of three major insular subregions (ventral anterior, dorsal anterior, and posterior). Considering the literature, we hypothesized that nicotine dependence would be negatively correlated with connectivity between anterior insula subregions and the ACC (i.e., participants with greater connectivity would show less dependence), and also with connectivity between the posterior insula and sensory-motor integration regions (e.g., supplementary motor area). We also hypothesized that dependence would be positively related to cue-induced activation in subregions of the insula, and that this activation would be related to insula RSFC patterns that are associated with dependence.

MATERIALS AND METHODS

Overview of experimental design

Functional magnetic resonance imaging (fMRI) data were collected during the resting state from adults who smoked cigarettes daily and maintained overnight abstinence before testing, which began between 8 and 9 a.m. (all scanning occurred prior to 11 a.m.). The study was part of a larger investigation on the brain correlates of smoking behavior and took place between September 2017 and March 2022. Data from a subsample of the participants were used in prior assessments [24, 49]. All participants in the prior resting state fMRI study as well as newly recruited ones were included in this study, which took place at the Semel Institute for Neuroscience and Human Behavior at the University of California, Los Angeles (UCLA). All study procedures were approved by the UCLA Institutional Review Board.

Participants

Two-hundred seventeen participants were recruited via online and print advertisements. They attended an intake session where they received a detailed explanation of the study procedures, provided written informed consent, and were screened for eligibility. Seventy met all study criteria and completed all procedures. Inclusion criteria were as follows: age of 18–45 years, generally good health, self-report of smoking at least 4 cigarettes per day for at least 1 year. Recent smoking history was verified during the intake session using a urine cotinine test (ACCUTEST Urine Cotinine Test, Jant Pharmacal Corp., Encino, CA, score ≥ 3 , cotinine ≥ 200 ng/ml). Exclusion criteria were positive urine tests for drugs of abuse other than nicotine or tetrahydrocannabinol, self-report of consuming ≥ 10 alcoholic drinks per week, any current psychiatric disorder other than TUD assessed via the Mini International Neuropsychiatric Interview for DSM-5 [50, 51], history of neurological injury, and using electronic cigarettes, cigars, snuff, or chewing tobacco > 3 times a month.

Verification of drug, alcohol abstinence and nicotine dependence

On the testing day, overnight (~12 h) abstinence from smoking was assessed with the Micro+ Smokerlyzer[®] breath carbon monoxide (CO) monitor (Bedford Scientific Ltd., Maidstone, Kent, UK). Participants were considered to have abstained on the day of testing if they either had a CO level of < 10 ppm or showed a 25% reduction from the CO measurement at the intake visit. Abstinence from cocaine, opiates, benzodiazepines, and amphetamines was verified with a five-panel urine drug test (Drugs of Abuse Test Insta-view[®], Alfa Scientific Designs Inc., Poway, CA). Alcohol abstinence was verified using a breathalyzer (Alco-Sensor FST[®], Intoximeters, Inc., St. Louis, MO). Recent abstinence from cannabis use was verified with the Dräger DrugTest[®] 5000 saliva test (Dräger, Inc., Houston, TX). Nicotine dependence was measured during the intake session using the FTND [52].

MRI data acquisition

All images were acquired on a 3-Tesla PRISMA (Siemens) MRI scanner using a 32-channel head coil receiver. The resting state imaging protocol consisted of

the continuous acquisition of 738 Echo-planar Image (EPI) volumes over a period of 9 min and 50 s. A multiband accelerated EPI pulse sequence (factor 8) was used, allowing us to acquire 72 axial slices during a repetition time (TR) of 800 ms with a 104×104 matrix. Resolution was $2 \times 2 \times 2$ mm³, echo time (TE) was 37 ms, and the flip angle was 52 degrees. Participants were asked to keep their eyes open and to look at a black screen during the resting state scan. For the fMRI task, a multi-echo EPI (ME-EPI) sequence was used (TE1 = 13.80 ms, TE2 = 35.94 ms, TE3 = 58.08 ms) with a multiband acceleration factor of four and Generalized Auto-calibrating Partially Parallel Acquisition acceleration factor of 2 (TR = 1.462 s, flip angle = 67 degrees, 280 volumes). Each volume consisted of 64 interleaved axial slices (2 mm cubic, 104×96 matrix). The multiecho sequence was used to increase the signal-to-noise ratio by reducing effects of non-TE dependent nuisance fluctuations such as motion and hardware instabilities [53] and by combining optimally the signals from the different echoes [54]. The structural T1-weighted images were obtained using a magnetization prepared rapid gradient echo sequence with the following parameters: isovoxel 0.8 mm³, FOV = 240×256 mm², TE = 2.24 ms, TR = 2400 ms; flip angle = 8°; 208 sagittal slices.

Cue-induced craving task

The task paradigm consisted of the presentation of short video clips, created by a professional film maker, that included both indoor and outdoor scenes in which young adults engaged in identical activities either while smoking (smoking cues) or not (neutral cues). These videos were used in two prior studies [55, 56]. Individuals in the videos were professional actors who provided consent for publication of their images. Six smoking cues and six neutral cues videos were presented. Each video clip was ~15 s in length (mean 14.97 ± 0.27) and was followed by a 1-s blank screen, after which participants were shown the following sentence: "What is your urge to smoke right now?". Participants had 10 s to indicate their response by using a trackball (Trackball2, Current Designs, Inc., Philadelphia, PA) to position the cursor on a radially arranged visual scale consisting of seven digits: "1" = "No urge", "7" = "Extreme urge" (see Supplementary Fig. 2 for schematic and further task details). After an 8-s inter-stimulus interval (ISI), the next video sequence was presented. Each trial, including the ISI, was ~34 s in duration. Video presentation order was pseudorandom across participants, such that number of consecutive videos of the same type (smoking, neutral) did not exceed three. The presentation and timing of all stimuli and collection of responses were programmed using Matlab (Mathworks, Natick, MA) and the Psychtoolbox (3.0.14, Rev. 8424) (www.psychtoolbox.org) on an Apple MacBook Pro laptop (MacOS 10.12.6, Apple Computers, Cupertino, CA). During scanning, visual stimuli were presented using a projector at the rear of the bore of the scanner, with participants viewing them via a mirror mounted on the head coil.

MRI data pre-processing

Image preprocessing for resting state data were mostly conducted with FSL (5.0.9). The initial stages included rigid body realignment to correct for head movements within each scanning run, skull removal, and non-linear registration to the Montreal Neurological Institute (MNI) template. Initial motion cleaning and noise reduction were performed using a 24-parameter linear regression model that included six motion parameters (3 translational dimensions along X, Y and Z axes and 3 rotational dimensions: "pitch", "roll" and "yaw"), the temporal derivatives of these parameters, and the quadratic of all parameters [57]. Mean frame displacement (FD) and the variance of signal change from the average signal (DVARS) of the raw images were estimated. A null sampling distribution of DVARS was used to identify frames with excessive variance at $p < 0.05$ [58]; frames with $FD > 0.45$ mm were also flagged. These frames as well as the one located in time just prior ($t - 1$) and two just after ($t + 1$ and $t + 2$) were included in a censoring temporal mask for data interpolation: a least-squares spectral decomposition of the uncensored data was performed to reconstitute data of the censored timepoints [see methods in [59]]. The uncensored data defined the frequency characteristics of signals that then replaced the censored data. This step aimed at minimizing the contamination of the signal from the censored frames during frequency filtering. The interpolated signal was then demeaned, detrended, and filtered using a bandpass filter (0.009–0.08 Hz), after which the interpolated timepoints were censored. Participants with $>50\%$ frames censored (i.e., those with <5 min of remaining resting state data) were excluded from analyses. To reduce the contribution from non-neuronal noise, the minimal number of principle components that explained at least 50% of the variance of mean signal extracted from white matter and cerebrospinal fluid were evaluated and regressed out from the signal [aCompCor50, [60]]. Volumes were then

spatially smoothed with a Gaussian filter using a 5-mm FWHM kernel. Each voxel was normalized to a mean value of 100 (SD = 1) to transform the data to Pearson's correlation coefficients (r).

The task-based fMRI data preprocessing differed slightly from that used for resting state data because of the ME-EPI sequence used. Data were first organized in the Brain Imaging Data Structure format [61] and processed using the fMRIPrep pipeline (version 20.2.5) for ME-EPI data [62]. Preprocessing was as follows: a reference volume and its skull-stripped version were generated from the shortest echo of the BOLD run using a custom method in fMRIPrep. The BOLD reference was then co-registered to the T1w reference using "bbregister" (FreeSurfer), which implements boundary-based registration. Co-registration was configured with six degrees of freedom. Head-motion parameters with respect to the BOLD reference (transformation matrices, and six corresponding rotation and translation parameters) were estimated before spatiotemporal filtering using FSL's MCFLIRT. BOLD runs were slice-time corrected using "3dTshift" (AFNI 20170207). The BOLD time-series (including slice-timing correction when applied) were resampled onto their original, native space by applying the transforms to correct for head-motion. A T2* map was estimated from the preprocessed BOLD images by fitting to a mono-exponential signal decay model with nonlinear regression, using T2*/S0 estimates from a log-linear regression fit as initial values. For each voxel, the maximal number of echoes with reliable signal in that voxel were used to fit the model. The calculated T2* map was then used to optimally combine preprocessed BOLD across echoes following the method described in [54]. The preprocessed BOLD time-series were then resampled into standard space (MNI152NLin2009cAsym) using the nonlinear registration calculated between the T1w image and a template (ANTs 2.1.0). The confounding time-series FD and DVARS were calculated based on the preprocessed BOLD images. Images with >0.5 mm FD or >1.5 standardized DVARS were annotated as motion outliers. All analyses were performed on Linux (CentOS release 6.10) using FSL (5.0.9), MATLAB (8.6), R (3.6.0) and FreeSurfer (6.0.0).

Resting-state fMRI seed-based analysis

To minimize bias, we used a statistically conservative voxel-wise whole-brain analytic approach rather than restricting to a priori-selected target regions or networks. On each of the two hemispheres of the brain, three insula seeds (ventral-anterior, dorsal-anterior, and posterior), were defined for RSFC analyses (Supplementary Fig. 1). To define the anterior insula, we compared anatomical landmarks from a probabilistic atlas [63] to RSFC-based parcellations of the insula [34, 35]. From these studies, we defined the ventral anterior insula parcel as the anterior inferior insular cortex (which includes the apex, the limen, and the transverse gyrus). The dorsal anterior insula was defined as the anterior and middle short gyri. The precentral sulcus was used to segment the anterior from the posterior insula. Using these landmarks, we manually determined the anterior insular subdivisions (dorsal and ventral, left and right) from the MNI152 template.

To evaluate RSFC between the insula seeds and other brain regions, the time series from each seed was extracted, and its first normalized eigen vector (mean = 100, SD = 1; to facilitate computation of Pearson's r) was used as a regressor in an ordinary least squares linear regression analysis on every voxel (as implemented in "film_gls" in FEAT). The parameter estimates of the model, corresponding to the Pearson's correlation coefficient (since data were previously normalized), were z-transformed to improve data normality.

The resulting z-transformed images were used in multi-level mixed effects models for group analyses with FMRIB's Local Analysis of Mixed Effects (FLAME1) with outlier deweighting, testing for the effect of nicotine dependence on RSFC for each seed. Specifically, two separate models were tested. The model included the total score of the FTND as the independent variable of interest.

To account for differences in motion during scanning between participants, the mean FD value was included as a covariate in all models, in addition to age. Results were cluster-corrected for multiple comparisons using a voxel-height threshold of $p < 0.001$ ($Z > 3.1$) and cluster threshold of $p < 0.05$ as recommended per Eklund et al. [64]. The coordinates reported here correspond to the peak voxel within a given cluster in MNI coordinate space.

Cue-induced craving task fMRI analysis

Individual preprocessed BOLD time-series were analyzed using the General Linear Model within FSL's FEAT (FSL 5.0.9). The design matrix used included four explanatory variables: (1) smoking and (2) non-smoking cues (i.e.,

Table 1. Participant characteristics for subgroups with resting state and cue-induced craving fMRI data.

Characteristic	Resting state fMRI		Cue-induced craving fMRI	
<i>N</i>	60		48	
Sex	32 M/28 F		24 M/24 F	
Ethnicity				
Not Hispanic or Latino	80.0%		79.2%	
Hispanic or Latino	15.0%		18.8%	
Unknown	5.0%		2.1%	
Race				
White	53.3%		54.2%	
Black/African	23.3%		25.0%	
Mixed	6.7%		4.2%	
Hawaiian/Pacific Islander	3.3%		4.2%	
Asian	1.7%		2.1%	
Unknown	11.7%		10.4%	
	Mean (range)	SD	Mean (range)	SD
Age (years)	32.8	7.1	32.9	7.3
Nicotine dependence (FTND ^a)	4.1 (0–9)	2.1	4.1 (0–9)	2.2
Tobacco/current use (cigarettes/day)	11.7	5.1	11.4	4.9
Tobacco/lifetime exposure (pack-years)	8.2	6.1	7.8	5.8
Alcohol consumption				
<i>N</i> with >0 drinks/week (drinks/week)	(<i>N</i> = 14) 5.8	2.5	(<i>N</i> = 12) 5.7	2.7
Cannabis consumption				
<i>N</i> with >0 gram/week (grams/week)	(<i>N</i> = 19) 4.4	4.6	(<i>N</i> = 15) 4.3	5.1
Craving ratings during cue presentation ^b				
Smoking cues			4.9	1.8
Neutral cues			4.0	1.7

Groups had overlapping participants and did not differ by age, ethnicity, race, FTND, cigarettes per day, or packs-years, alcohol and cannabis consumption (*t*-test, *ps* > 0.05).

^aFagerström Test of Nicotine Dependence.

^bCraving ratings significantly differed across cue-types (*t*-test, *ps* < 0.05).

videos), and the rating phase after (3) smoking and (4) non-smoking cues. Delta functions for each variable were defined as (1) the start and end of each video presentation and (2) the onset of the rating prompt followed by the time in which the response was made. These boxcar shaped delta functions were then convolved with a double gamma HRF function and used as the explanatory variables. The 24 motion parameters estimated during preprocessing were included in the model, as were all frames flagged as motion outliers. Low frequency fluctuation of the signal was removed using a 200-s high-pass filter. The contrast images of the model were spatially smoothed with a 5 mm FWHM kernel. The contrast of smoking cues minus neutral cues was used for the group analysis. To parallel the RS seed analysis, we performed region of interest analyses of contrast estimates. The same a priori-defined insular subregions used as seeds for the resting state analyses (Supplementary Fig. 1) were assessed using the General Linear Model in Jamovi [65] with age and mean frame displacement (mFD) as covariates. We also performed a voxel wise whole brain group-level mixed-effects analysis (FLAME1 with outlier deweighting). The FTND score for each participant was used in this model, as well as age and mFD. Statistical maps reflecting (1) the mean effect of smoking cue and (2) the influence of nicotine dependence (FTND) on this effect were cluster-corrected for multiple comparisons (voxel height threshold: $Z > 3.1$ ($p < 0.001$), cluster significance $p < 0.05$). All analyses at the group level were performed and reported in MNI space.

RESULTS

Participant characteristics

Seventy two adults who endorsed daily cigarette smoking (and met study inclusion criteria) underwent resting state fMRI scanning.

Among this group, twelve subjects were excluded for not meeting abstinence criteria ($N = 7$) or had excessive motion during the rest scan ($N = 5$). The final sample of participants with resting state data included 60 individuals whose characteristics (sex, age, level of nicotine dependence, cigarette use, and exposure) are shown in Table 1. The same group of 60 participants received the cue-induced craving task; however, nine participants were excluded due to technical problems during scanning (i.e., behavioral response equipment failures and visual display issues), and three participants were excluded for excessive motion (>0.5 mm FD). In all, data from 48 participants were used in the final analysis of task fMRI data—all of whom also received resting state scans. Table 1 shows participant characteristics for participants whose cue-induced craving task data were used; characteristics did not significantly differ from the resting state sample ($ps > 0.5$).

RSFC of insular subregions and cue-induced activation

Examining the mean connectivity of each insular subregion, we found a distinction between anterior and posterior insula connectivity patterns, but very little difference between ventral and dorsal anterior insula connectivity (Supplementary Fig. 3). With respect to the primary anterior insula connectivity target that was related to FTND—the superior parietal lobule (SPL) (see results below)—we observed significant RSFC of all anterior insular seeds with SPL at our default threshold ($p < 0.001$), except for the correlation with the left ventral anterior seed, which was significant at $p < 0.01$.

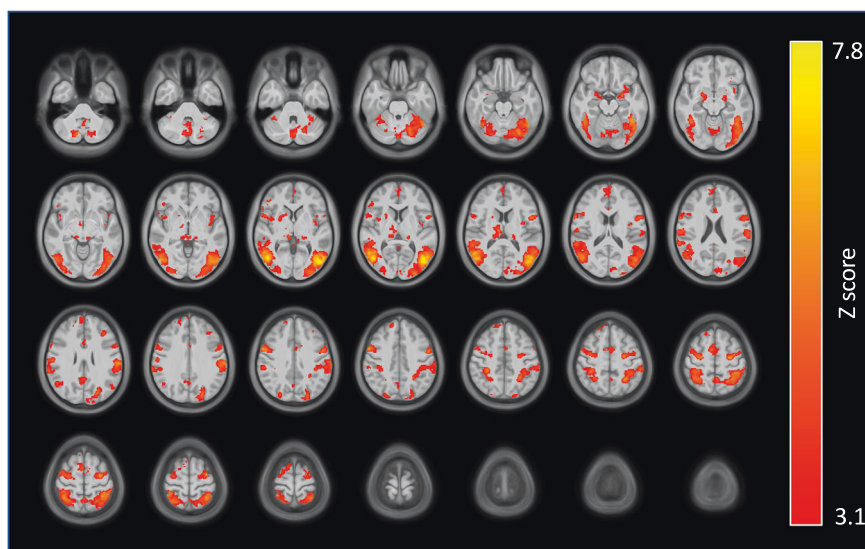


Fig. 1 Whole-brain, voxel-wise cluster-corrected results from the contrast of smoking vs. neutral cues. Regions of activation included amygdala, occipito-temporal cortex, medial prefrontal cortex, frontal eye fields, intraparietal sulcus, superior parietal lobule, and insula (mostly posterior). Figure shows thresholded statistical map ($Z > 3.1$ ($p < 0.001$), cluster corrected) displayed on the average of spatially normalized T1-weighted images across participants ($N = 48$). Brain images are presented in radiological convention (right = left).

Whole-brain voxel-wise results from the contrast of smoking vs. neutral cues indicated several regions of activation, including amygdala, occipito-temporal cortex, medial prefrontal cortex, frontal eye fields, intraparietal sulcus, and SPL (mainly within the precuneus), and insula (Fig. 1). Insula clusters were found in mostly anterior but some posterior left and right subregions.

Nicotine dependence and RSFC of insular subregions

Testing the association of the FTND total score with RSFC between the insula seeds and the rest of the brain revealed relationships for the anterior but not posterior insular seeds. The connectivity target regions were mostly in the SPL for all anterior seed regions, and only negative relationships were found (Table 2 and Fig. 2). Specifically, we observed negative relationships between FTND and RSFC of the left and right dorsal and left ventral anterior insula with medial portions of the SPL, including the left precuneus ($x = -10$, $y = -72$, $z = 50$), and more lateral areas of the SPL. The left ventral anterior insula also showed the precuneus target when assessed at an uncorrected threshold ($p < 0.001$). For both the left and right ventral and right dorsal anterior insula seeds, a common lateral SPL target was observed ($x = 28$, $y = -50$, $z = 70$).

Nicotine dependence and cue-induced activation in insular subregions

Region-of-interest analyses of the a priori-defined insular subregions indicated that cue-induced activation in the right and left dorsal anterior insula showed positive correlations with FTND ($p < 0.05$, Table 3). These effects would not survive the Bonferroni correction for the six a priori tests and should therefore be cautiously interpreted. The whole-brain voxel-wise analysis revealed a positive correlation of nicotine dependence with cue-induced activation in the left middle frontal gyrus (Supplementary Fig. 4). Specifically, the interaction of cue-type (smoking/neutral) and FTND showed clusters in this region. Using an uncorrected threshold ($p < 0.001$ uncorrected for cluster size), we observed a cluster (18 contiguous voxels) within the left anterior dorsal insula ($X = -32$, $Y = 10$, $Z = 4$; peak $Z = 4.16$). We observed no negative relationships between FTND and activation from the smoking vs. neutral cues contrast, nor did we observe significant relationships between craving ratings during the task (i.e., mean smoking minus

mean neutral cue ratings, mean of all cues combined) and insular activation (Table 1).

Post hoc analysis of FTND items with insular RSFC and cue-induced activation

To determine if specific item(s) from the FTND questionnaire drove the relationships between the FTND total score and insular RSFC and cue-induced activation, we conducted several post hoc analyses that included responses to each of the six FTND items in the same model, including age and mean FD as covariates. Separate models were run for each insular subregion and each of the two imaging outcomes (RSFC, activation). For RSFC, three FTND items significantly correlated negatively with insula-SPL RSFC (Supplementary Table 1). The first FTND item (FTND1), assessing the time until the first cigarette of the day after waking, was significantly related to RSFC of all insular subregions with SPL, whereas the fourth item (FTND4), assessing the number of cigarettes smoked per day, was significantly related to bilateral dorsal anterior and left ventral anterior insula RSFC with SPL (Supplementary Fig. 5). The third item (FTND3), asking whether participants hate to give up cigarettes smoked in the morning vs. other times, was only significantly negatively associated with dorsal anterior RSFC with SPL. For cue-induced activation, all insular subregions significantly correlated positively with the 5th item (FTND5), assessing whether or not participants smoke more frequently during the first hours after waking than during the rest of the day. In addition, activation in the left ventral anterior insula showed a significant correlation with FTND4.

Relationship between insular RSFC and cue-induced activation

We completed an additional post hoc analysis to determine whether RSFC of anterior insula seeds and the SPL are related to cue-induced activation within the respective anterior insular subregions. Mean RSFC of each seed and its SPL target were used as independent variables in four separate linear models, using the smoking vs. neutral cue contrast estimates (averaged within each seed) as dependent variables (controlling for age and mFD). We found that the activation of the left dorsal anterior insula was negatively correlated with RSFC between the left dorsal anterior insula and the SPL ($p < 0.013$; Fig. 3 and Supplementary Table 2).

Table 2. Correlation of nicotine dependence (FTND scores) with resting state functional connectivity and cue-induced activation of insular subregions.

Seed	Connectivity target/ activation cluster ^a	Laterality	Cluster volume (voxels)	Z (max) ^b	X ^c	Y ^c	Z ^c
Correlation of FTND with resting state functional connectivity of insular subregions							
Left dorsal anterior insula							
	Superior parietal lobule/ Precuneus	L	133	4.91	-10	-72	50
	Postcentral sulcus	L	80	4.22	-40	-34	46
Right dorsal anterior insula							
	Superior parietal lobule	R	236	4.19	22	-50	66
	Superior parietal lobule (Precuneus)	L	141	5.34	-10	-72	50
	Superior parietal lobule	L	129	4.33	-28	-46	66
	Superior parietal lobule (Precuneus)	R	107	4.59	6	-58	62
	Precentral gyrus	R	73	4.66	20	-12	68
Left ventral anterior insula							
	Precentral gyrus	L	171	4.48	-52	4	44
	Superior parietal lobule (Intraparietal sulcus/Precuneus)	L	170	4.61	-14	-68	52
	Superior parietal lobule	R	143	4.35	28	-50	70
Right ventral anterior insula							
	Superior parietal lobule	R	113	4.35	28	-50	70
Correlation of FTND with cue-induced fMRI activation (smoking cues vs. neutral cues)							
	Middle frontal gyrus	L	115	4.5	-28	38	18

Whole-brain voxel-wise resting state functional connectivity targets and smoking cue-induced fMRI activation clusters are presented. All results were cluster corrected (voxel height: $Z > 3.1$ ($p < 0.001$), cluster threshold: $p < 0.05$).

^aAnatomical labels determined via parcellations from the atlas by Destrieux et al. [87].

^bZ-statistic of peak voxel.

^cMNI coordinates of peak voxel within cluster.

Controlling for cannabis co-use and effects of sex

Since a portion (one-third) of the participants were co-users of cannabis, we conducted post hoc analyses to determine if the RSFC and cue-induced activation results were influenced by cannabis use. We included days of cannabis use in the last 30 days and amount used per week as covariates in a linear model for each insular subregion to determine effects on connectivity and cue-induced activation. We also examined effects of sex given known sex differences in the relationship between nicotine dependence and cigarette craving and in anterior insular thickness [24]. No significant effects were found for any of these covariates (Supplementary Table 3).

DISCUSSION

This study showed relationships between nicotine dependence and RSFC of subregions within the anterior insula. Specifically, seed-based whole-brain RSFC analyses, using six insular subregions as seeds, indicated a negative association with connectivity of the anterior insula and the SPL. The precuneus, a region along the medial wall of the SPL, and a cluster in the right lateral SPL were the most common connectivity targets among the anterior insula seeds that showed a relationship with dependence. Moreover, we observed a positive relationship between cue-induced activation in the dorsal anterior insula and nicotine dependence, and an inverse relationship was observed between activation in this region and RSFC with SPL. A subset of FTND items primarily drove the FTND relationships for all or some of insular subregional RSFC with SPL and cue-induced activation.

These results suggest potential targets for neuromodulation studies. Specifically, modulation of RSFC in anterior insula-SPL circuits, by stimulating the anterior insula, SPL, or intermediary regions connecting this circuit, may potentially impact nicotine dependence. In this regard, promising results from LIFUP stimulation of subcortical regions indicate modulation of cortical networks, illustrating impact of stimulation of a local region on its related circuitry [66]. The cue-induced activation results also suggest that the dorsal anterior insula may be a potential target for modulating the craving response in those who have relatively high levels of nicotine dependence. Whether modulation of these targets can impact nicotine dependence and craving remains to be empirically determined.

Although we hypothesized a relationship between nicotine dependence and connectivity of anterior insula subregions with limbic regions and components of the salience network (i.e., ACC), we found a relationship with connectivity to SPL regions, brain areas that are not included among limbic or salience network structures but are involved in cognitive and affective function. The precuneus has been associated with self-referential processing, empathy, and episodic memory retrieval [67], and has a central role in the default mode network [68, 69]. It is a primary brain region activated during smoking cue-induced activation, as indicated by meta-analyses [70]. Precuneus activation during presentation of smoking- and alcohol-related cues was positively associated with nicotine and alcohol dependence, respectively [71]. Moreover, in individuals who smoke cigarettes, anterior insula-precuneus connectivity, similar to the connectivity pattern observed in this study, was correlated with cue-induced craving

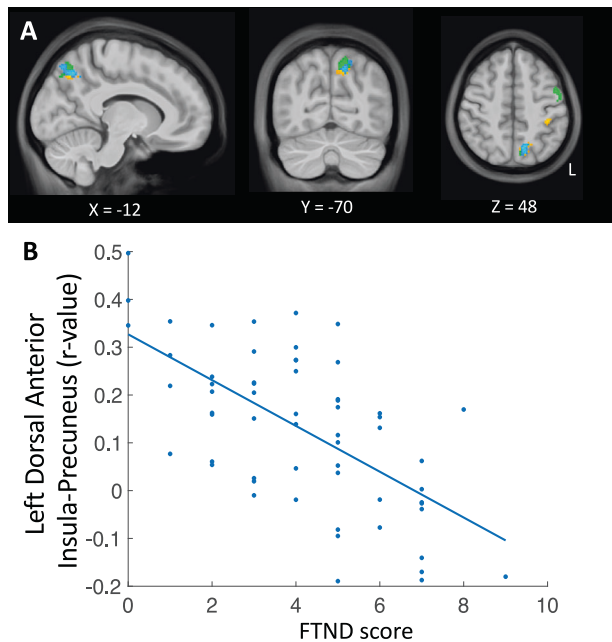


Fig. 2 Relationship between nicotine dependence (FTND total score) and anterior insula-superior parietal lobule functional connectivity. FTND total score correlated negatively with connectivity of several insular subregions and clusters within the superior parietal lobule (SPL). Figure shows thresholded statistical maps [voxel height: $Z > 3.1$ ($p < 0.001$), cluster threshold: $p < 0.05$] indicating insula connectivity targets in left precuneus/SPL. Insula seeds are represented by different colors: left (orange) and right (blue) dorsal anterior insula and left (green) ventral anterior insula (the overlapping cluster from the right ventral anterior insula seed is not shown). Results are summarized in Table 2. Brain images are presented in radiological convention (right=left) (“L” in figure indicates left side of the brain). **B** Scatterplot of data extracted from left precuneus cluster (blue in **A**) from the left dorsal anterior insula connectivity maps of individual participants are shown along with linear fit to illustrate the negative direction of the relationship between FTND and functional connectivity. The data points appeared similarly for connectivity other anterior insula seed regions.

Table 3. Correlation of nicotine dependence (FTND scores) with cue-induced activation (smoking vs. neutral cues) of insular subregions.

Insula subregion	SS	F	p	Effect size (η^2p)
L dorsal anterior	3777	6.75	0.012 ^a	0.133
R dorsal anterior	1641	5.08	0.029 ^a	0.104
L ventral anterior	1301	2.27	0.139	0.049
R ventral anterior	854	2.17	0.148	0.047
L posterior	490	1.21	0.278	0.027
R posterior	538	1.82	0.184	0.040

Statistical values for each subregion are from separate linear models that included age and mean FD as covariates. General linear model details in “Methods”.

SS sums of squares.

^aStatistically significant at $p < 0.05$.

[72]. Both the prior and current findings suggest a role for the interaction of the precuneus with the anterior insula in maintenance of nicotine dependence, especially aspects that involve self-referential processes. The lateral SPL and the precuneus showed similar effects. With its role in visual-spatial attention [73, 74], weakened anterior insula connectivity with

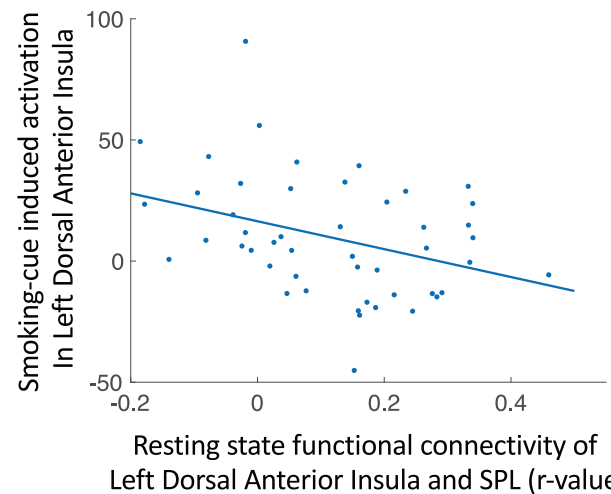


Fig. 3 Relationship between left dorsal anterior insula-SPL resting state functional connectivity and cue-induced activation (smoking vs. neutral cues) in the same insular subregion ($p < 0.013$). Further statistics are provided in Supplementary Table 2.

lateral SPL in those with higher levels of dependence may reflect disrupted coordination of attentional processing during periods of abstinence.

The regional specificity of the relationship between nicotine dependence and RSFC of anterior vs. posterior insula suggests that nicotine dependence is more associated with affective/cognitive vs. somatosensory aspects of interoception. Given the role of the posterior insula as the “primary interoceptive cortex” [43, 44], receiving input about somatosensory states of the body, our findings suggest that dependence is not significantly associated with these primary interoceptive functions, but mostly with higher order affective/cognitive domains served by the anterior insula [39, 40]. Example cognitive aspects of interoception involved in nicotine dependence may include linking bodily sensations related to craving to planning for nicotine consumption (e.g., determining the next occasion to smoke), and affective aspects may include generation of negative affective states based on bodily sensations related to brief abstinence/withdrawal.

Our results are partially consistent with previous insula RSFC studies of nicotine dependence, which found associations with the ACC. One study of young participants (15–24 years old) who did not abstain from smoking prior to scanning found a negative relationship between anterior insula-ACC RSFC and nicotine dependence [29]. However, ACC was selected as the connectivity target of interest post hoc, based on an analysis that showed greater anterior insula-ACC connectivity in individuals who smoked vs. those who did not. Another study similarly found a negative association between dependence and insula-ACC connectivity [31], but it used the whole, bilateral insula as a seed, eliminating the possibility of differentiating effects based on subregions and laterality. Lastly, a third study found a negative relationship between nicotine dependence and posterior insula-ACC connectivity in individuals with schizophrenia, as well as those without psychiatric diagnoses [30]. The current study may not have found significant results involving the ACC due to differences in analytic methodology. We used whole-brain voxel-wise RSFC analyses with strict multiple comparison correction. Yet, even when lowering the voxel-height threshold to $p < 0.05$ (from $p < 0.001$), we did not find significant clusters within the ACC after applying cluster-based correction. Another possible reason for the absence of a positive ACC finding may be our use of rigorous motion-cleaning approaches [59, 75, 76]—considered essential for removing artifacts that may lead to spurious correlations [77]. The use of a simultaneous multi-slice sequence may have been

another point of discrepancy with previous findings, especially given the relatively high multiband factor (MB = 8) used. Although spatial biases in correlations due to noise amplification in seed-based RSFC analyses increases with higher MB factors, application of temporal filtering, as we have done here, decreases these biases [78]. Despite the possibility of reduced effect sizes with temporal filtering, we did not observe results in ACC, even with lower statistical thresholds. Direct comparisons of single- and multi-band acquisition sequences with various factors would be needed to determine the potential effects of MR acquisition parameters on our findings.

We found a relationship between cue-induced activation and dependence in bilateral dorsal anterior insula, considered important for updating motivational states with respect to specific actions [40]. The relationship we observed suggests that the region is more sensitive to switching between appetitive stimuli (i.e., smoking cues) and neutral stimuli in those who are more dependent on nicotine.

Our cue-induced activation findings disagree slightly with those of prior studies. One study found a relationship of nicotine dependence with cue-induced activation in the right posterior insula when comparing cues vs. baseline (similar contrast used in our study), and in left anterior and posterior insula in a comparison of responses to smoking vs. food cues [32]. In addition, we did not find a relationship between nicotine dependence and cue-induced activation in the precuneus as previously observed [71]. These discrepancies may be due to a number of factors related to differences in neuroimaging methods and analytic practices. These include stricter statistical thresholding procedures adopted by the neuroimaging community since the publication of the earlier studies [64] as well as greater noise reduction offered by multi-echo BOLD imaging acquisition and preprocessing approaches used here [54].

Analysis of the FTND items revealed that some contributed significantly to relationships with RSFC. Time until the first cigarette of the day and number of cigarettes per day were associated with RSFC of most anterior insula subregions with SPL (right ventral anterior insula RSFC was not related to cigarettes per day). These two FTND items comprise the Heaviness of Smoking Index, another measure that predicts success of smoking cessation [79, 80]. Anterior insula-SPL RSFC may contribute to aspects of nicotine dependence that influence success of smoking cessation. We also observed a strong relationship between cue-induced anterior insula (all subregions) and frequency of smoking during the first hours after waking. Although the implications of this finding are not entirely clear, cognitive/affective aspects of interoception served by the anterior insula may be related to a sense of urgency to smoke.

Observation of a negative relationship between left dorsal anterior insula-SPL RSFC and cue-induced activation in the same subregion is in line with the assumption that those with greater nicotine dependence (lower anterior insula-SPL RSFC) would respond more strongly to smoking cues (i.e., have greater craving) during brief abstinence than those with less dependence. This link between “spontaneous” anterior insula-SPL RSFC and cue-induced activation suggests that dorsal anterior insula circuitry may be an important target for addressing both nicotine dependence and craving.

Brain stimulation is currently viewed as a promising therapy for smoking cessation [81, 82] and studies targeting the insula have demonstrated mixed success in affecting smoking-related variables, such as craving and withdrawal [13, 16]. TMS has received clearance by the U.S. Food and Drug Administration for smoking cessation [83], and while several studies have shown encouraging results, including one indicating that high-frequency deep TMS to the insula and prefrontal cortex reduces nicotine dependence [84], others have shown weak or no effects [13, 45]. By highlighting the relevance of insular subregional RSFC patterns, which are weaker in strength in those who have greater nicotine dependence, this work provides additional relevant targets for future stimulation

studies. For example, stimulation studies may not only choose to target the anterior insula, but also regions within the SPL with the aim of increasing RSFC within the relevant circuitry we've identified. Although it is not known whether such anatomical specificity is important for successful therapeutic outcomes, our results suggest this possibility. Stimulation techniques that provide greater spatial resolution (e.g., LIFUP) than TMS would be required to test this specificity. We did not find effects of co-use of cannabis and sex, suggesting that therapeutic interventions would be effective for those who use other substances in addition to nicotine and robust across the sexes.

This study is limited in that it cannot determine whether weak insular connectivity is a cause or consequence of nicotine dependence although pre-clinical studies have suggested a potential causal role of insular connectivity on dependence. In a data-driven study of rats, an insular-frontal network was predictive of later nicotine dependence [85]. It remains to be determined if a similar finding will emerge from longitudinal human studies, such as the Adolescent Brain Cognitive Development study [86].

Overall, we provide evidence for the association of nicotine dependence with weak RSFC and greater cue-induced activation of distinct insula subregions, mainly, dorsal anterior insula-right SPL connectivity and dorsal anterior insula activation, respectively. This regional specificity within the insula highlights the heterogeneity of the insula with respect to neural processes involved in maintenance of smoking and suggests multiple potential targets for brain-based therapies that address nicotine addiction.

DATA AVAILABILITY

All self-report, toxicology, and summary fMRI data discussed in this manuscript, as well as the code used for statistical analyses, are publicly available from the Open Science Framework web site under project title, “Nicotine dependence and functional connectivity and activation of insular cortex subregions” (<https://osf.io/24tkf/>).

REFERENCES

1. World Health Organization. WHO global report on trends in prevalence of tobacco use 2000–2025. 4th ed. Geneva: World Health Organization; 2019.
2. Hughes JR, Keely J, Naud S. Shape of the relapse curve and long-term abstinence among untreated smokers. *Addiction*. 2004;99:29–38.
3. Gómez-Coronado N, Walker AJ, Berk M, Dodd S. Current and emerging pharmacotherapies for cessation of tobacco smoking. *Pharmacotherapy*. 2018;38:235–58.
4. Rosen LJ, Galili T, Kott J, Goodman M, Freedman LS. Diminishing benefit of smoking cessation medications during the first year: a meta-analysis of randomized controlled trials. *Addiction*. 2018;113:805–16.
5. Baker TB, Piper ME, Smith SS, Bolt DM, Stein JH, Fiore MC. Effects of combined varenicline with nicotine patch and of extended treatment duration on smoking cessation: a randomized clinical trial. *JAMA*. 2021;326:1485–93.
6. Heatherton TF, Kozlowski LT, Frecker RC, Fagerström KO. The Fagerström Test for Nicotine Dependence: a revision of the Fagerström Tolerance Questionnaire. *Br J Addict*. 1991;86:1119–27.
7. Killen JD, Fortmann SP, Kraemer HC, Varady A, Newman B. Who will relapse? Symptoms of nicotine dependence predict long-term relapse after smoking cessation. *J Consult Clin Psychol*. 1992;60:797–801.
8. Pekel Ö, Ergör G, Günay T, Baydur H, Choussein B, Budak R, et al. Smoking cessation and the effect of nicotine dependence on relapse rate in Izmir, Turkey. *Turkish J Med Sci*. 2015;45:895–901.
9. Ikonomidis I, Thymis J, Kourea K, Kostelli G, Neocleous A, Katogiannis K, et al. Fagerstrom score predicts smoking status six months after hospitalization for acute myocardial infarction: a prospective study. *Hell J Cardiol*. 2022;67:28–35.
10. Zhang T, Wang L, Xu Z, Zhang Q, Ye Y. Predictors of smoking relapse after percutaneous coronary intervention in Chinese patients. *J Clin Nurs*. 2018;27:e951–58.
11. Polańska K, Hanke W, Sobala W. Smoking relapse one year after delivery among women who quit smoking during pregnancy. *Int J Occup Med Environ Health*. 2005;18:159–65.
12. United States Public Health Service Office of the Surgeon General; National Center for Chronic Disease Prevention and Health Promotion (US) Office on Smoking and Health. Chapter 3. New biological insights into smoking cessation. Smoking cessation: a report of the surgeon general [Internet]. Washington (DC): US Department of Health and Human Services; 2020.

13. Antonelli M, Fattore L, Sestito L, Di Giuda D, Diana M, Addolorato G. Transcranial magnetic stimulation: a review about its efficacy in the treatment of alcohol, tobacco and cocaine addiction. *Addict Behav.* 2021;114:106760.
14. Mahoney JJ 3rd, Hanlon CA, Marshalek PJ, Rezai AR, Krinke L. Transcranial magnetic stimulation, deep brain stimulation, and other forms of neuromodulation for substance use disorders: review of modalities and implications for treatment. *J Neurol Sci.* 2020;418:117149.
15. Ibrahim C, Rubin-Kahana DS, Pushparaj A, Musiol M, Blumberger DM, Daskalakis ZJ, et al. The insula: a brain stimulation target for the treatment of addiction. *Front Pharmacol.* 2019;10:720.
16. Regner MF, Tregellas J, Kluger B, Wylie K, Gowin JL, Tanabe J. The insula in nicotine use disorder: functional neuroimaging and implications for neuromodulation. *Neurosci Biobehav Rev.* 2019;103:414–24.
17. Abdolahi A, Williams GC, Benesch CG, Wang HZ, Spitzer EM, Scott BE, et al. Damage to the insula leads to decreased nicotine withdrawal during abstinence. *Addiction.* 2015;110:1994–2003.
18. Gaznick N, Tranel D, McNutt A, Bechara A. Basal ganglia plus insula damage yields stronger disruption of smoking addiction than basal ganglia damage alone. *Nicotine Tob Res.* 2014;16:445–53.
19. Naqvi NH, Rudrauf D, Damasio H, Bechara A. Damage to the insula disrupts addiction to cigarette smoking. *Science.* 2007;315:531–34.
20. Suñer-Soler R, Grau A, Gras ME, Font-Mayolas S, Silva Y, Dávalos A, et al. Smoking cessation 1 year poststroke and damage to the insular cortex. *Stroke.* 2012;43:131–36.
21. Lin F, Wu G, Zhu L, Lei H. Region-specific changes of insular cortical thickness in heavy smokers. *Front Hum Neurosci.* 2019;13:265.
22. Wang C, Huang P, Shen Z, Qian W, Li K, Luo X, et al. Gray matter volumes of insular subregions are not correlated with smoking cessation outcomes but negatively correlated with nicotine dependence severity in chronic smokers. *Neurosci Lett.* 2019;696:7–12.
23. Morales AM, Ghahremani D, Kohno M, Helleman GS, London ED. Cigarette exposure, dependence, and craving are related to insula thickness in young adult smokers. *Neuropsychopharmacology.* 2014;39:1816–22.
24. Perez Diaz M, Pochon JB, Ghahremani DG, Dean AC, Faulkner P, Petersen N, et al. Sex differences in the association of cigarette craving with insula structure. *Int J Neuropsychopharmacol.* 2021;24:624–33.
25. Fedota JR, Stein EA. Resting-state functional connectivity and nicotine addiction: prospects for biomarker development. *Ann N Y Acad Sci.* 2015;1349:64.
26. Sutherland MT, McHugh MJ, Pariyadath V, Stein EA. Resting state functional connectivity in addiction: lessons learned and a road ahead. *Neuroimage.* 2012;62:2281–95.
27. Li S, Yang Y, Hoffmann E, Tyndale RF, Stein EA. CYP2A6 genetic variation alters striatal-cingulate circuits, network hubs, and executive processing in smokers. *Biol Psychiatry.* 2017;81:554–63.
28. Hong LE, Hodgkinson CA, Yang Y, Sampath H, Ross TJ, Buchholz B, et al. A genetically modulated, intrinsic cingulate circuit supports human nicotine addiction. *Proc Natl Acad Sci USA.* 2010;107:13509–14.
29. Bi Y, Yuan K, Guan Y, Cheng J, Zhang Y, Li Y, et al. Altered resting state functional connectivity of anterior insula in young smokers. *Brain Imaging Behav.* 2017;11:155–65.
30. Moran LV, Sampath H, Stein EA, Hong LE. Insular and anterior cingulate circuits in smokers with schizophrenia. *Schizophr Res.* 2012;142:223–29.
31. Zhou S, Xiao D, Peng P, Wang SK, Liu Z, Qin HY, et al. Effect of smoking on resting-state functional connectivity in smokers: an fMRI study. *Respirology.* 2017;22:1118–24.
32. Claus ED, Blaine SK, Filbey FM, Mayer AR, Hutchison KE. Association between nicotine dependence severity, BOLD response to smoking cues, and functional connectivity. *Neuropsychopharmacology.* 2013;38:2363–72.
33. McClernon FJ, Kozink RV, Rose JE. Individual differences in nicotine dependence, withdrawal symptoms, and sex predict transient fMRI-BOLD responses to smoking cues. *Neuropsychopharmacology.* 2008;33:2148–57.
34. Chang LJ, Yarkoni T, Khaw MW, Sanfey AG. Decoding the role of the insula in human cognition: functional parcellation and large-scale reverse inference. *Cereb Cortex.* 2013;23:739–49.
35. Deen B, Pitskel NB, Pelphrey KA. Three systems of insular functional connectivity identified with cluster analysis. *Cereb Cortex.* 2011;21:1498–506.
36. Uddin LQ. *Saliency network of the human brain.* Academic Press; 2016.
37. Kurth F, Zilles K, Fox PT, Laird AR, Eickhoff SB. A link between the systems: functional differentiation and integration within the human insula revealed by meta-analysis. *Brain Struct Funct.* 2010;214:519–34.
38. Gu X, Liu X, Van Dam NT, Hof PR, Fan J. Cognition-emotion integration in the anterior insular cortex. *Cereb Cortex.* 2013;23:20–7.
39. Touroutoglou A, Hollenbeck M, Dickerson BC, Feldman Barrett L. Dissociable large-scale networks anchored in the right anterior insula subserve affective experience and attention. *Neuroimage.* 2012;60:1947–58.
40. Wager TD, Barrett LF. From affect to control: functional specialization of the insula in motivation and regulation. *BioRxiv.* 2017:102368.
41. Wang Y, Zhu L, Zou Q, Cui Q, Liao W, Duan X, et al. Frequency dependent hub role of the dorsal and ventral right anterior insula. *Neuroimage.* 2018;165:112–17.
42. Janes AC, Krantz NL, Nickerson LD, Frederick BB, Lukas SE. Craving and cue reactivity in nicotine-dependent tobacco smokers is associated with different insula networks. *Biol Psychiatry Cogn Neurosci Neuroimaging.* 2020;5:76–83.
43. Craig AD. Interoception: the sense of the physiological condition of the body. *Curr Opin Neurobiol.* 2003;13:500–5.
44. Critchley HD, Wiens S, Rotshtein P, Ohman A, Dolan RJ. Neural systems supporting interoceptive awareness. *Nat Neurosci.* 2004;7:189–95.
45. Hauer L, Scarano GI, Brigo F, Golaszewski S, Lochner P, Trinka E, et al. Effects of repetitive transcranial magnetic stimulation on nicotine consumption and craving: a systematic review. *Psychiatry Res.* 2019;281:112562.
46. Arulpragasam AR, van 't Wout-Frank M, Barredo J, Faucher CR, Greenberg BD, Philip NS. Low intensity focused ultrasound for non-invasive and reversible deep brain neuromodulation—a paradigm shift in psychiatric research. *Front Psychiatry.* 2022;13:825802.
47. Addicott MA, Sweitzer MM, Froeliger B, Rose JE, McClernon FJ. Increased functional connectivity in an insula-based network is associated with improved smoking cessation outcomes. *Neuropsychopharmacology.* 2015;40:2648–56.
48. Fedota JR, Ding X, Matous AL, Salmeron BJ, McKenna MR, Gu H, et al. Nicotine abstinence influences the calculation of salience in discrete insular circuits. *Biol Psychiatry Cogn Neurosci Neuroimaging.* 2018;3:150–59.
49. Ghahremani DG, Pochon JB, Perez Diaz M, Tyndale RF, Dean AC, London ED. Functional connectivity of the anterior insula during withdrawal from cigarette smoking. *Neuropsychopharmacology.* 2021;46:2083–89.
50. Sheehan DV, Lecrubier Y, Sheehan KH, Amorim P, Janavs J, Weiller E, et al. The Mini-International Neuropsychiatric Interview (MINI): the development and validation of a structured diagnostic psychiatric interview for DSM-IV and ICD-10. *J Clin Psychiatry.* 1998;59 Suppl 20:22–33.
51. Hergueta T, Weiller E. Evaluating depressive symptoms in hypomanic and manic episodes using a structured diagnostic tool: validation of a new Mini International Neuropsychiatric Interview (MINI) module for the DSM-5'With Mixed Features' specifier. *Int J Bipolar Disord.* 2013;1:21.
52. Fagerström K. Determinants of tobacco use and renaming the FTND to the Fagerström Test for Cigarette Dependence. *Nicotine Tob Res.* 2011;14:75–8.
53. Kundu P, Inati SJ, Evans JW, Luh WM, Bandettini PA. Differentiating BOLD and non-BOLD signals in fMRI time series using multi-echo EPI. *Neuroimage.* 2012;60:1759–70.
54. Posse S, Wiese S, Gembris D, Mathiak K, Kessler C, Grosse-Ruyken ML, et al. Enhancement of BOLD-contrast sensitivity by single-shot multi-echo functional MR imaging. *Magn Reson Med.* 1999;42:87–97.
55. Ghahremani DG, Faulkner P, Cox CM, London ED. Behavioral and neural markers of cigarette-craving regulation in young-adult smokers during abstinence and after smoking. *Neuropsychopharmacology.* 2018;43:1616–22.
56. Do KT, Galván A. Neural sensitivity to smoking stimuli is associated with cigarette craving in adolescent smokers. *J Adolesc Health.* 2016;58:186–94.
57. Satterthwaite TD, Elliott MA, Gerraty RT, Ruparel K, Loughhead J, Calkins ME, et al. An improved framework for confound regression and filtering for control of motion artifact in the preprocessing of resting-state functional connectivity data. *Neuroimage.* 2013;64:240–56.
58. Afyouni S, Nichols TE. Insight and inference for DVARS. *Neuroimage.* 2018;172:291–312.
59. Power JD, Mitra A, Laumann TO, Snyder AZ, Schlaggar BL, Petersen SE. Methods to detect, characterize, and remove motion artifact in resting state fMRI. *Neuroimage.* 2014;84:320–41.
60. Muschelli J, Nebel MB, Caffo BS, Barber AD, Pekar JJ, Mostofsky SH. Reduction of motion-related artifacts in resting state fMRI using aCompCor. *Neuroimage.* 2014;96:22–35.
61. Gorgolewski KJ, Auer T, Calhoun VD, Craddock RC, Das S, Duff EP, et al. The brain imaging data structure, a format for organizing and describing outputs of neuroimaging experiments. *Sci Data.* 2016;3:160044.
62. Esteban O, Markiewicz CJ, Blair RW, Moodie CA, Isik AI, Erramuzpe A, et al. fMRIPrep: a robust preprocessing pipeline for functional MRI. *Nat Methods.* 2019;16:111–16.
63. Failenlot I, Heckemann RA, Frot M, Hammers A. Macroanatomy and 3D probabilistic atlas of the human insula. *Neuroimage.* 2017;150:88–98.
64. Eklund A, Nichols TE, Knutsson H. Cluster failure: why fMRI inferences for spatial extent have inflated false-positive rates. *Proc Natl Acad Sci USA.* 2016;113:7900–05.
65. The jamovi project (2022). jamovi (Version 2.3) [Computer Software]. Retrieved from <https://www.jamovi.org>.
66. Cain JA, Visagan S, Johnson MA, Crone J, Blades R, Spivak NM, et al. Real time and delayed effects of subcortical low intensity focused ultrasound. *Sci Rep.* 2021;11:6100.

67. Cavanna AE, Trimble MR. The precuneus: a review of its functional anatomy and behavioural correlates. *Brain*. 2006;129:564–83.
68. Utevsky AV, Smith DV, Huettel SA. Precuneus is a functional core of the default-mode network. *J Neurosci*. 2014;34:932–40.
69. Fransson P, Marrelec G. The precuneus/posterior cingulate cortex plays a pivotal role in the default mode network: evidence from a partial correlation network analysis. *Neuroimage*. 2008;42:1178–84.
70. Engelmann JM, Versace F, Robinson JD, Minnix JA, Lam CY, Cui Y, et al. Neural substrates of smoking cue reactivity: a meta-analysis of fMRI studies. *Neuroimage*. 2012;60:252–62.
71. Courtney KE, Ghahremani DG, London ED, Ray LA. The association between cue-reactivity in the precuneus and level of dependence on nicotine and alcohol. *Drug Alcohol Depend*. 2014;141:21–6.
72. Moran-Santa Maria MM, Hartwell KJ, Hanlon CA, Canterbury M, Lematty T, Owens M, et al. Right anterior insula connectivity is important for cue-induced craving in nicotine-dependent smokers. *Addiction Biol*. 2015;20:407–14.
73. Molenberghs P, Mesulam MM, Peeters R, Vandenberghe RR. Remapping attentional priorities: differential contribution of superior parietal lobule and intraparietal sulcus. *Cereb Cortex*. 2007;17:2703–12.
74. Wang J, Yang Y, Fan L, Xu J, Li C, Liu Y, et al. Convergent functional architecture of the superior parietal lobule unraveled with multimodal neuroimaging approaches. *Hum Brain Mapp*. 2015;36:238–57.
75. Power JD, Schlaggar BL, Petersen SE. Recent progress and outstanding issues in motion correction in resting state fMRI. *Neuroimage*. 2015;105:536–51.
76. Siegel JS, Power JD, Dubis JW, Vogel AC, Church JA, Schlaggar BL, et al. Statistical improvements in functional magnetic resonance imaging analyses produced by censoring high-motion data points. *Hum Brain Mapp*. 2014;35:1981–96.
77. Power JD, Barnes KA, Snyder AZ, Schlaggar BL, Petersen SE. Spurious but systematic correlations in functional connectivity MRI networks arise from subject motion. *Neuroimage*. 2012;59:2142–54.
78. Risk BB, Murden RJ, Wu J, Nebel MB, Venkataraman A, Zhang Z, et al. Which multiband factor should you choose for your resting-state fMRI study? *Neuroimage*. 2021;234:117965.
79. Borland R, Yong HH, O'Connor RJ, Hyland A, Thompson ME. The reliability and predictive validity of the Heaviness of Smoking Index and its two components: findings from the International Tobacco Control Four Country study. *Nicotine Tob Res*. 2010;Suppl 12:S45–50.
80. Baker TB, Piper ME, McCarthy DE, Bolt DM, Smith SS, Kim SY, et al. Time to first cigarette in the morning as an index of ability to quit smoking: implications for nicotine dependence. *Nicotine Tob Res*. 2007;Suppl 4:S555–70.
81. Grall-Bronnec M, Sauvaget A. The use of repetitive transcranial magnetic stimulation for modulating craving and addictive behaviours: a critical literature review of efficacy, technical and methodological considerations. *Neurosci Biobehav Rev*. 2014;47:592–613.
82. Petit B, Dornier A, Meille V, Demina A, Trojak B. Non-invasive brain stimulation for smoking cessation: a systematic review and meta-analysis. *Addiction*. 2022;117:2768–79.
83. Young JR, Galla JT, Appelbaum LG. Transcranial magnetic stimulation treatment for smoking cessation: an introduction for primary care clinicians. *Am J Med*. 2021;134:1339–43.
84. Dinur-Klein L, Dannon P, Hadar A, Rosenberg O, Roth Y, Kotler M, et al. Smoking cessation induced by deep repetitive transcranial magnetic stimulation of the prefrontal and insular cortices: a prospective, randomized controlled trial. *Biol Psychiatry*. 2014;76:742–9.
85. Hsu LM, Keeley RJ, Liang X, Brynildsen JK, Lu H, Yang Y, et al. Intrinsic insular-frontal networks predict future nicotine dependence severity. *J Neurosci*. 2019;39:5028–37.
86. Bjork JM, Straub LK, Provost RG, Neale MC. The ABCD study of neurodevelopment: Identifying neurocircuit targets for prevention and treatment of adolescent substance abuse. *Curr Treat Options Psychiatry*. 2017;4:196–209.
87. Destrieux C, Fischl B, Dale A, Halgren E. Automatic parcellation of human cortical gyri and sulci using standard anatomical nomenclature. *Neuroimage*. 2010;53:1–15.

ACKNOWLEDGEMENTS

The authors thank Ms. Andrea Donis, Ms. Diana Paez, Ms. Citlaly Cahuantzi, Ms. Tinisha Sakhani, and Mr. Hector Diaz, whose contribution to data collection helped make this work possible.

AUTHOR CONTRIBUTIONS

All authors were involved in designing the study and contributed to writing the manuscript. DGG and MPD acquired the data. J-BFP, DGG, MPD and ACD were responsible for data analysis. RFT contributed to decisions regarding participant characterization. DGG, J-BFP and EDL drafted the manuscript. As principal investigator of the study, EDL is accountable for all aspects of the work, including its accuracy and integrity. All authors have reviewed and approve the final version of this manuscript.

FUNDING

This research was supported, in part, by a grant from the National Institute on Drug Abuse (NIDA) (R37 DA044467, EDL) and endowments from the Thomas P. and Katherine K. Pike Chair in Addiction Studies and the Marjorie M. Greene Trust (EDL). MPD was supported by a Ruth L. Kirschstein Postdoctoral Individual National Research Award from NIDA (F32 DA049500-01A1). We acknowledge the Canada Research Chairs program (RFT, the Canada Research Chair in Pharmacogenomics).

COMPETING INTERESTS

RFT has consulted for Quinn Emanuel and Ethismos Research Inc. All other authors declare no conflicts of interest.

ADDITIONAL INFORMATION

Supplementary information The online version contains supplementary material available at <https://doi.org/10.1038/s41386-023-01528-0>.

Correspondence and requests for materials should be addressed to Dara G. Ghahremani or Edythe D. London.

Reprints and permission information is available at <http://www.nature.com/reprints>

Publisher's note Springer Nature remains neutral with regard to jurisdictional claims in published maps and institutional affiliations.



Open Access This article is licensed under a Creative Commons Attribution 4.0 International License, which permits use, sharing, adaptation, distribution and reproduction in any medium or format, as long as you give appropriate credit to the original author(s) and the source, provide a link to the Creative Commons license, and indicate if changes were made. The images or other third party material in this article are included in the article's Creative Commons license, unless indicated otherwise in a credit line to the material. If material is not included in the article's Creative Commons license and your intended use is not permitted by statutory regulation or exceeds the permitted use, you will need to obtain permission directly from the copyright holder. To view a copy of this license, visit <http://creativecommons.org/licenses/by/4.0/>.

© The Author(s) 2023